Formation and Spectroscopic Characterization of Chelated d^0 Yttrium(III)−Alkyl−Alkene Complexes

Charles P. Casey,* Susan L. Hallenbeck,* J. Monty Wright, and Clark R. Landis*

Contribution from the Department of Chemistry, University of Wisconsin, Madison, Wisconsin 53706

Received September 16, 1996. Revised Manuscript Received May 14, 1997[⊗]

Abstract: The yttrium hydride dimer $(Cp^*_2YH)_2$ (**2**) reacted rapidly with 3,3-dimethyl-1,4-pentadiene in methylcyclohexane-d_{14} at −78 °C to form the d^0 yttrium(III) pentenyl chelate complex $Cp^*_2Y[\eta^1,\eta^2\text{-}CH_2CH_2C(CH_3)_2CH{=}CH_2]$ (**4**). Low-temperature ^1H, ^{13}C, and ^1H NOESY NMR spectroscopy of **4** established bonding of the tethered alkene to the d^0 metal center. Quantitative analysis of the NOESY time course using the Conformer Population Analysis method demonstrates that the dominant conformers in solution are interconverting pairs of chelated complexes, one in a twist-boat conformation and the other a chair conformer. No significant contribution by a free alkene conformation is required to explain the spectroscopic data. Addition of THF to pentenyl chelate **4** at −78 °C displaced the alkene and formed the yttrium(III) pentenyl THF adduct $Cp^*_2Y[\eta^1\text{-}CH_2CH_2C(CH_3)_2CH{=}CH_2](THF)$ (**5**), in which there is no interaction between the pendant alkene and the d^0 metal center. Yttrium hydride dimer **2** also reacted with either 1,4-pentadiene or methylenecyclobutane to form the same pentenyl chelate complex $Cp^*_2Y[\eta^1,\eta^2\text{-}CH_2CH_2CH_2CH{=}CH_2]$ (**6**). The interconversion of deuterium-labeled chelate complexes **6**-1,1,5,5-d_4 and **6**-3,3,5,5-d_4 at −78 °C ($\Delta G^{\ddagger} = 14.4 \pm 0.2$ kcal mol^{-1}) establishes that intramolecular alkene insertion is occurring under the reaction conditions.

Introduction

Coordination of an alkene to an electron-deficient metal−alkyl complex has been proposed as a requisite chain propagation step in Ziegler−Natta alkene polymerization.[1−3] Subsequent alkyl migration to the coordinated α-alkene via a four-center transition state generates a new C−C bond and forms a vacant coordination site *cis* to the growing polymer chain. The key d^0 metal−alkyl−alkene intermediate is expected to be unstable due to the absence of π-backbonding and the rapid insertion. For example, ethylene binding energies between 7 and 11 kcal mol^{-1} have been calculated for a series of neutral Ti(IV) halides,[4] and experimental values for the activation barrier for the addition of ethylene to the Ti−C bond of $Cp_2TiCH_3^+$ range from 6 to 12 kcal mol^{-1}.[5] As a result, metal−alkyl−alkene complexes in active polymerization systems have only been observed for non-d^0 metal catalysts. The d^6 cobalt(III) alkyl ethylene complex $Cp^*[P(OMe)_3]CoCH_2CH_3(H_2C{=}CH_2)^+$ was detected by low-temperature ^{13}C NMR spectroscopy under an ethylene atmosphere.[6] Similarly, d^8 Pd(II)(diimine)(alkyl)(alkene)$^+$ complexes were detected by low-temperature ^1H NMR spectroscopy during alkene polymerization.[7]

d^0 transition metal−alkene complexes have been directly observed in only a few cases.[8−12] For example, the pentadienyl ligand of the d^0 zirconocene(IV) complex $[((Me_3C)C_5H_4)_2Zr(\eta^1,\eta^2,\eta^2\text{-}CH_2C(Me){=}C(Me)C(Me){=}CHMe)]^+[B(4\text{-}C_6H_4F)_4]^-$ binds to zirconium through a σ-bond and two weak η^2-alkene interactions.[10d] Jordan recently reported the synthesis of the zirconium(IV) oxypent-4-enyl chelate complex $[Cp_2Zr(\eta^1,\eta^2\text{-}OC(CH_3)_2CH_2CH_2CH{=}CH_2)]^+[MeB(C_6F_5)_3]^-$ (**1**), which was designed to model a cationic $(Cp_2Zr{-}alkyl{-}alkene)^+$ intermediate.[12] Binding of the tethered alkene of **1** was observed in solution by NMR spectroscopy and in the solid state by X-ray crystallography.

⊗ Abstract published in *Advance ACS Abstracts,* September 15, 1997.

(1) (a) Cossee, P. *J. Catal.* **1964**, *3*, 80. (b) Arlman, E. J. *J. Catal.* **1964**, *3*, 89. (c) Arlman, E. J.; Cossee, P. *J. Catal.* **1964**, *3*, 99.

(2) (a) Brookhart, M.; Green, M. L. H. *J. Organomet. Chem.* **1983**, *250*, 395. (b) Brookart, M.; Green, M. L. H.; Pardy, R. B. A. *J. Chem. Soc., Chem. Commun.* **1983**, 691.

(3) For a recent review of stereospecific homogeneous olefin polymerization, see: Brintzinger, H. H.; Fischer, D.; Mülhaupt, R.; Rieger, B.; Waymouth, R. M. *Angew. Chem., Int. Ed. Engl.* **1995**, *34*, 1143.

(4) Jensen, V. R.; Ystenes, M.; Wärnmark, K.; Åkermark, B.; Sevensson, M.; Siegbahn, P. E. M.; Bloomberg, M. R. A. *Organometallics* **1994**, *13*, 282 and references therein.

(5) (a) Natta, G.; Pasquon, I. *Adv. Catal.* **1959**, *11*, 1. (b) Machon, J. P.; Hermant, R.; Houteaux, J. P. *J. Polym. Sci. Symp.* **1975**, *52*, 107. (c) Chien, J. C. W. *J. Am. Chem. Soc.* **1959**, *81*, 86.

(6) Brookhart, M.; Volpe, A. F.; Lincoln, D. M.; Horváth, I. T.; Millar, J. M. *J. Am. Chem. Soc.* **1990**, *112*, 5634.

(7) (a) Rix, F. C.; Brookhart, M.*J. Am. Chem. Soc.* **1995**, *117*, 5634. (b) Johnson, L. K.; Mecking, S.; Brookhart, M. *J. Am. Chem. Soc.* **1996**, *118*, 267.

(8) Alkali metal−alkene complexes: (a) Klein, H.-F.; Witty, H.; Schubert, U. *J. Chem. Soc., Chem. Commun.* **1983**, 231. (b) Klein, H.-F.; Grob, J.; Basset, J.-M.; Schubert, U. *Z. Naturforsch* **1980**, *35b*, 614. (c) Goddard, R.; Krüger, C.; Pörschke, K. L.; Wilke, G. *J. Organomet. Chem.* **1986**, *308*, 85. (d) Schade, C.; von Ragué Schleyer, P. *Adv. Organomet. Chem.* **1987**, *27*, 167. (e) Smart, J. B.; Hogan, R.; Scherr, P. A.; Emerson, M. T.; Oliver, J. P. *J. Organomet. Chem.* **1974**, *64*, 1.

(9) Main group metal−alkene complexes: (a) Jonas, K. *Adv. Organomet. Chem.* **1981**, *19*, 97. (b) Dolzine, T. W.; Oliver, J. P. *J. Am. Chem. Soc.* **1974**, *96*, 1737. (c) Albright, M. J.; Denis, J. N. St.; Oliver, J. P. *J. Organomet. Chem.* **1977**, *125*, 1. (d) Hata, G. *J. Chem. Soc., Chem. Commun.* **1968**, 7.

(10) d^0 transition metal−alkene complexes: (a) Kress, J.; Osborn, J. A. *Angew. Chem., Int. Ed. Engl.* **1992**, *31*, 1585. (b) Nolan, S. P.; Marks, T. J. *J. Am. Chem. Soc.* **1989**, *111*, 8538. (c) Burns, C. J.; Andersen, R. A. *J. Am. Chem. Soc.* **1987**, *109*, 915. (d) Horton, A. D.; Orpen, A. G. *Organometallics* **1992**, *11*, 8. (e) Ballard, D. G. H.; Burnham, D. R.; Twose, D. L. *J. Catal.* **1976**, *44*, 116. (f) Wolczanski, P. T.; Bennet, J. L. *J. Am. Chem. Soc.* **1994**, *116*, 2179.

(11) For attempted detection of tethered d^0 transition metal−alkene complexes, see: (a) Gagnè, M. R.; Stern, C. L.; Marks, T. J. *J. Am. Chem. Soc.* **1992**, *114*, 275. (b) Lehmkuhl, H.; Tsien, Y.-L.; Jannsen, E.; Mynott, R. *Chem. Ber.* **1983**, *116*, 2426. (c) Clark, R. J. H.; Coles, M. A. *J. Chem. Soc., Dalton Trans.* **1974**, 1462. (d) Clark, R. J. H.; Stockwell, J. A.; Wilkins, J. D. *J. Chem. Soc., Dalton Trans.* **1976**, 120.

(12) Wu, Z.; Jordan, R. F.; Petersen, J. L. *J. Am. Chem. Soc.* **1995**, *117*, 5867.

S0002-7863(96)03256-8 CCC: $14.00

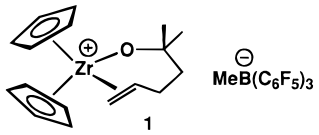

1

Due to the relevance of d^0 metal−alkyl−alkene complexes to alkene polymerization and the lack of suitable model complexes, we sought to generate d^0 metal−alkyl−alkene complexes which would model the alkene intermediate present in α-alkene polymerization. Here we report the synthesis and solution structure of a series of d^0 yttrium(III) pentenyl complexes which possess a coordinated alkene. We began by investigating the reaction of the yttrium hydride dimer $(Cp^*_2YH)_2$ (**2**)[13,14] with 3,3-dimethyl-1,4-pentadiene. Yttrium was chosen because group III metallocene−alkyl−alkene complexes are neutral and because of possible advantages from spin $^1/_2$ ^{89}Y (100% abundance). The 4-pentenyl side chain was chosen to favor alkene complexation by the chelation effect, and the *gem*-dimethyl group was incorporated into the pentenyl backbone to promote ring-forming chelation.[15] Intramolecular alkene insertion is endothermic by >4 kcal mol^{-1} due to the 26 kcal mol^{-1} strain in the resulting methylcyclobutyl complex.[16]

Results

Synthesis of Yttrium(III) Pentenyl Chelate Complex $Cp^*_2YCH_2CH_2C(CH_3)_2CH{=}CH_2$ (4). The yttrium hydride dimer $(Cp^*_2YH)_2$ (**2**) was prepared *in situ* by hydrogenation of the monomeric yttrium(III) metallocene complex $Cp^*_2YCH(SiMe_3)_2$ (**3**) in methylcyclohexane-d_{14} at 0 °C.[13] A colorless solution of **2** reacted rapidly with 3,3-dimethyl-1,4-pentadiene in methylcyclohexane-d_{14} at −78 °C to form a bright yellow solution of the d^0 yttrium(III) pentenyl chelate complex $Cp^*_2Y[\eta^1,\eta^2\text{-}CH_2CH_2C(CH_3)_2CH{=}CH_2]$ (**4**) (Scheme 1). **4** was formed in 98 ± 5% yield as determined by ^{1}H NMR spectroscopy using $CH_2(SiMe_3)_2$ obtained from cleavage of **3** as an internal standard. Pentenyl chelate complex **4** was also prepared in toluene-d_8 in 84% yield by ^{1}H NMR spectroscopy. **4** was stable for more than 2 weeks at −78 °C but decomposed after several hours at −50 °C. Due to the thermal instability of **4**, the complex was characterized without isolation by ^{1}H and ^{13}C NMR spectroscopy at −100 °C.

In the ^{1}H NMR spectrum of **4**, methylene resonances at δ −0.44 (br s, $\omega_{1/2}$ = 20 Hz, YCH_2) and 1.84 (br s, $\omega_{1/2}$ = 12 Hz, YCH_2CH_2) confirmed the addition of yttrium hydride to one of the diene double bonds. A single resonance at δ 1.93 was observed for the Cp* ligands, and a resonance at δ 1.03 was assigned to the *gem*-dimethyl group of the pentenyl chain (Supporting Information Figure 1). The substantial differences between the vinyl hydrogen chemical shifts in tethered metal−alkene complex **4** and in the starting diene provided evidence for coordination of the pendant alkene to the d^0 yttrium center (Table 1, Supporting Information Figure 2). The chemical shift difference (Δδ) between the terminal vinyl hydrogens of **4** is 1.38 ppm (δ 3.76, d, J_{cis} = 10.7 Hz; δ 5.14, d, J_{trans} = 17.8 Hz), but the chemical shift difference is only 0.05 ppm (δ 4.87, d, J_{cis} =10.5 Hz; δ 4.92, d, J_{trans} = 17.3 Hz) in the starting diene. The secondary vinyl hydrogen of **4** (δ 6.78, dd) is shifted 1.04 ppm to substantially higher frequency than in the starting diene (δ 5.74, dd). The similarity between the vinyl coupling constants of **4** and the starting diene suggest that the carbon−carbon double bond of chelate complex **4** is relatively unperturbed. No significant change in the chemical shift of the vinyl resonances was observed over the concentration range 20−70 mM, which indicates that the percentage of coordinated alkene is constant. This is consistent with complete intramolecular coordination of the alkene to the d^0 metal center.

Scheme 1

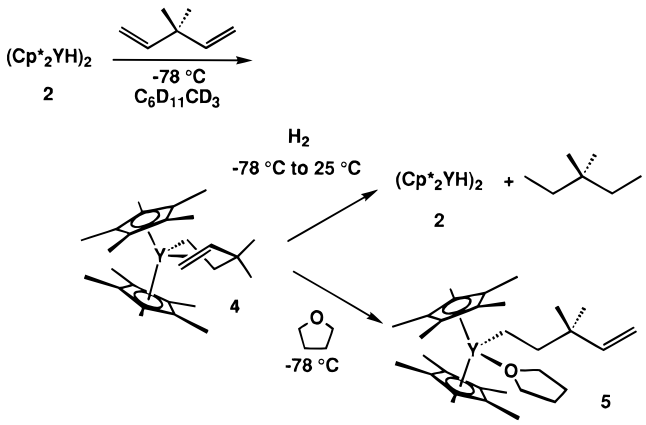

In the ^{13}C NMR spectrum of **4**, methylene resonances at δ 33.7 (d, J_{YC} = 45.8 Hz, YCH_2) and 14.9 (YCH_2CH_2) confirmed the formation of an alkylyttrium complex. The magnitude of the Y−C coupling constant is similar to the values reported for the asymmetric methylyttrium dimer $(Cp^*_2YCH_3)_2$ (^{13}C NMR, −80 °C, toluene: δ 22.0, $^1J_{YC}$ = 42.7 Hz; δ 21.8, $^1J_{YC}$ = 51.1 Hz).[17] In contrast, the YCH_2 resonance for the symmetrically bridged butylyttrium dimer $[(C_5H_4Me)_2Y(CH_2)_3CH_3]_2$ appears as a triplet, with $^1J_{YC}$ = 23.0 Hz.[14a]

Resonances at δ 11.6 and 116.3 were assigned to the Cp* methyl and Cp* ring carbon atoms of **4**, respectively, and a resonance at δ 43.1 was assigned to the *gem*-dimethyl group of the pentenyl chain. The 15 ppm shift to higher frequency of the resonance of the internal alkene carbon atom of **4** (δ 161.1, d, J_{CH} = 151 ± 2 Hz) relative to that in 3,3-dimethyl-1,4-pentadiene (δ 146.1, d, J_{CH} = 151 Hz) provided evidence for alkene coordination (Table 1). The chemical shift of the terminal alkene carbon atom of **4** (δ 110.5, t, J_{CH} = 154 ± 2 Hz) is similar to that of the starting diene (δ 111.1, J_{CH} = 156 Hz). The similarity of the vinyl J_{CH} coupling constants of **4** and the starting diene is inconsistent with an agostic Y−H−C interaction in **4**.[2a] The ^{1}H and ^{13}C NMR chemical shifts for the complexed alkene of **4** suggest that the double bond is bound asymmetrically to the d^0 yttrium center and that the internal alkene carbon atom is positively polarized. The alkene resonances of **4** closely resemble the chemical shifts reported by Jordan for the complexed alkene in zirconium(IV) oxypent-4-enyl chelate complex **1**.[12]

A static chelate structure for **4** would possess diastereotopic Cp* groups and diastereotopic *gem*-methyl groups. Therefore, the observation of resonances for equivalent Cp* and *gem*-methyl groups in both the ^{1}H and ^{13}C NMR spectra suggests that a fluxional process interconverts the enantiomers of **4**. Migration of yttrium from one alkene enantioface to the other is the minimum required process (Scheme 2). This can be accomplished by dissociation of the chelated alkene to generate

(13) (a) den Haan, K. H.; de Boer, J. L.; Teuben, J. H.; Spek, A. L.; Kojic-Prodic, B.; Hays, G. R.; Huis, R. *Organometallics* **1986**, *5*, 1726. (b) den Haan, K. H.; Wielstra, Y.; Teuben, J. H. *Organometallics* **1987**, *6*, 2053.

(14) For alkene polymerization reactions catalyzed by yttrium(III) metallocenes, see: (a) Ballard, D. G. H.; Courtis, A.; Holton, J.; McMeeking, J.; Pearce, R. *J. Chem. Soc., Chem. Commun.* **1978**, 994. (b) Coughlin, E. B.; Bercaw, J. E. *J. Am. Chem. Soc.* **1992**, *114*, 7606.

(15) Kirby, A. J. *Adv. Phys. Org. Chem.* **1980**, *17*, 183.

(16) A preliminary communication has appeared: Casey, C. P.; Hallenbeck, S. L.; Pollock, D. W.; Landis, C. R. *J. Am. Chem. Soc.* **1995**, *117*, 9770.

(17) Watson, P. L. *J. Am. Chem. Soc.* **1983**, *105*, 6491.

Table 1. Comparison of Alkene Resonances for **4**−**6**, 3,3-Dimethyl-1,4-pentadiene, and 1,4-Pentadiene[a]

	^{1}H NMR (500 MHz)			^{13}C NMR (91 Mhz) and ^{13}C{^{1}H} NMR (126 MHz)	
compound	δ (=CH_2)	Δd (=CH_2)	δ (−CH=)	δ (=CH_2)	δ (−CH=)
3,3-dimethyl-1,4-pentadiene	4.87 (d, J = 10.5 Hz), 4.92 (d, J = 17.3 Hz)	0.05	5.74 (dd, J = 17.3, 10.5 Hz, −CH=)	111.1 (J_{CH} = 156 Hz)	146.1 (J_{CH} = 151 Hz)
4	3.76 (d, J = 10.7 Hz), 5.14 (d, J = 17.8 Hz)	1.38	6.78 (dd, J = 17.8, 10.7 Hz, −CH=)	110.5 (J_{CH} = 154 ± 2 Hz)	161.1 (J_{CH} = 151 ± 2 Hz)
5	4.75 (m, 2 H)	∼0.0	5.78 (dd, J = 17.8, 10.9 Hz, −CH=)	108.4	150.7
1,4-pentadiene	5.00 (m, 2 H)	∼0.0	5.75 (m)	115.8	135.8
6	3.79 (d, J = 10.0 Hz), 5.25 (d, J = 17.5 Hz)	1.46	6.58 (m)	112.9	158.1

[a] All spectra were obtained in $C_6D_{11}CD_3$ at −100 °C.

Scheme 2

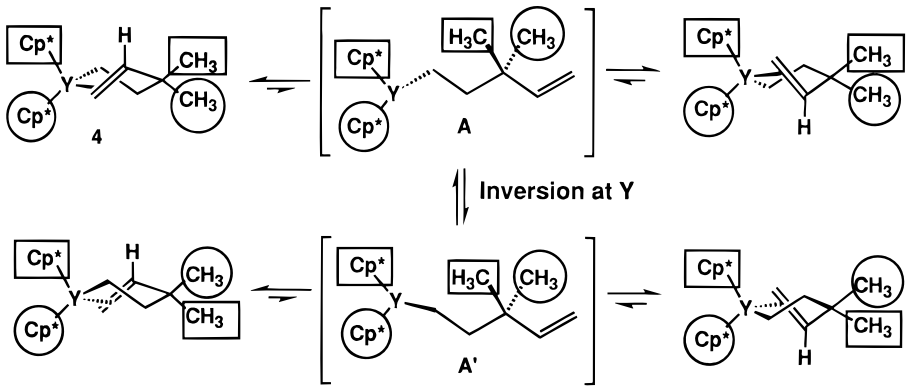

the η^1-intermediate Cp*$_2$Y[η^1-$CH_2CH_2C(CH_3)_2CH$=CH_2] (**A**), followed by recoordination to the opposite face of the alkene. Alternatively, this could occur by nondissociative migration of yttrium to the opposite alkene enantioface via a carbon−hydrogen σ-bond intermediate.[18] Migration of yttrium to the opposite alkene enantioface interchanges the relationships of the Cp* and *gem*-dimethyl groups relative to the secondary vinyl hydrogen whether or not inversion at yttrium takes place. Inversion at yttrium (**A** ↔ **A′**) changes the relationship between the Cp* and Me groups (Scheme 2). The rapidity of the fluxional process at −100 °C is consistent with the expected weakness of a d^0 metal−alkene interaction.

Variable-temperature studies revealed no significant change in the chemical shifts of the vinyl resonances between −100 and −50 °C. This indicates that chelate complex **4** is strongly favored over **A** throughout this temperature range. No change in the chemical shift or peak width of the YCH_2 resonance was observed over the same temperature range.

The Y−C bond of **4** was hydrogenated at −78 °C under 2 atm of H_2 to form yttrium hydride dimer **2** and 3,3-dimethylpentane (Scheme 1). The organic fragment was characterized by ^{1}H and ^{13}C NMR spectroscopy and by GC/MS analysis.

Synthesis of Yttrium(III) Pentenyl THF Adduct Cp*$_2$Y-[η^1-$CH_2CH_2C(CH_3)_2CH$=CH_2](THF) (5). The possibility that the unusual vinyl chemical shifts of **4** might be due to the proximity of yttrium rather than alkene complexation was tested by making a THF complex with a dangling alkene side chain. Addition of THF to a solution of **4** in methylcyclohexane-d_{14} at −78 °C led to immediate displacement of the coordinated alkene and formation of a colorless solution of the 1:1 yttrium(III) pentenyl THF adduct Cp*$_2$Y[η^1-$CH_2CH_2C(CH_3)_2CH$=CH_2](THF) (**5**) (Scheme 1). **5** was formed in 97 ± 5% yield by ^{1}H NMR spectroscopy using $CH_2(SiMe_3)_2$ as an internal standard (Cp* resonance versus $SiMe_3$). Complex **5** was thermally unstable and was characterized without isolation by ^{1}H and ^{13}C NMR spectroscopy at −100 °C. The ^{1}H and ^{13}C NMR shifts for the carbon−carbon double bond of **5** suggest that there is no interaction between the pendant alkene and the d^0 metal center.

In the ^{1}H NMR spectrum of **5**, the α- and β-CH_2 resonances of coordinated THF were observed at δ 3.64 and 1.35, respectively (free THF: δ 3.62, 1.76). The chemical shift of the terminal vinyl hydrogens of **5** (δ 4.75, 2 H, m) was similar to the shifts observed for 3,3-dimethyl-1,4-pentadiene (δ 4.87, 1 H, d; 4.92, 1 H, d; $\Delta\delta$ = 0.05 ppm) (Table 1, Supporting Information Figure 3). In contrast, the chemical shifts of the terminal vinyl hydrogens of the complexed alkene in **4** were considerably different (δ 3.76, d; 5.24, d; $\Delta\delta$ = 1.38 ppm). The secondary vinyl hydrogen of **5** is observed at δ 5.78, which is also very similar to the chemical shift for the secondary hydrogen in the starting diene (δ 5.74) and very different from the corresponding resonance for chelate **4** (δ 6.78). The YCH_2 (δ −0.74) and Cp* (δ 1.88) resonances were shifted slightly to lower frequency compared to the resonances for chelate complex **4** (δ −0.44, YCH_2; δ 1.93, Cp*).[19] The resonance corresponding to the *gem*-dimethyl group of the pentenyl chain was observed at δ 0.90

The ^{13}C NMR spectrum of **5** displayed resonances at δ 67.7 and 25.7 corresponding to the α- and β-CH_2 resonances, respectively, of the coordinated THF (free THF: δ 67.5, 26.0). The ^{13}C NMR chemical shifts of the alkene carbon atoms (δ 108.4, =CH_2; 150.7, CH=) of **5** are similar to those of 3,3-dimethyl-1,4-pentadiene and very different from those observed for **4** (Table 1). Resonances at δ 33.7 (d, J_{YC} = 50.3 Hz, YCH_2) and 14.7 (YCH_2CH_2) were assigned to the α- and β-CH_2 resonances of the pentenyl chain, respectively. Significantly, the yttrium−carbon coupling was 5 Hz larger than that in chelated complex **4**.[19a] Resonances at δ 11.6 and 115.2 were

(18) Peng, T.-S.; Gladysz, J. A. *J. Am. Chem. Soc.* **1992**, *114*, 4174.

(19) (a) den Haan, K. H.; Wielstra, Y.; Eshuis, J. J. W.; Teuben, J. H. *J. Organomet. Chem.* **1987**, *323*, 181. (b) Evans, W. J.; Meadows, J. H.; Hunter, W. E.; Atwood, J. L. *J. Am. Chem. Soc.* **1984**, *106*, 1291.

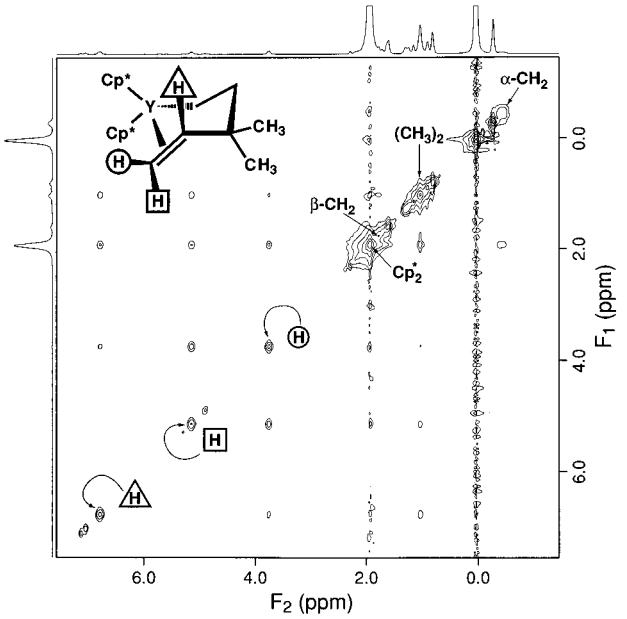

Figure 1. ^{1}H NOESY spectrum of $Cp^*_2Y[\eta^1,\eta^2\text{-}CH_2CH_2C(CH_3)_2\text{-}CH{=}CH_2]$ (**4**) in $C_6D_{11}CD_3$ at −100 °C (τ_m = 75 ms).

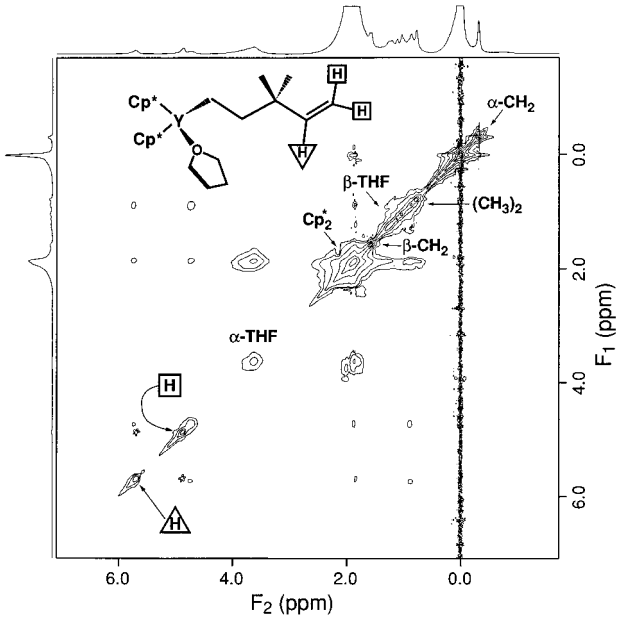

Figure 2. ^{1}H NOESY spectrum of $Cp^*_2Y[\eta^1\text{-}CH_2CH_2C(CH_3)_2\text{-}CH{=}CH_2](THF)$ (**5**) in $C_6D_{11}CD_3$ at −100 °C (τ_m = 75 ms). Excess 3,3-dimethyl-1,4-pentadiene is observed at δ 4.87, 4.92 (=CH_2), and 5.74 (CH=).

assigned to the Cp* methyl and Cp* ring carbon atoms, respectively, and a resonance at δ 43.5 was assigned to the *gem*-dimethyl group of the pentenyl chain.

Comparison of NOE Spectra of 4 and 5. The proximity of the pendant alkene to the d^0 metal center in pentenyl chelate complex **4** was confirmed by a steady-state 1D NOE NMR experiment. When the Cp* resonance at δ 1.93 and the β-CH_2 resonance at δ 1.84 were irradiated for 40 ms (0.008 mT), NOEs of $-8 \pm 2\%$ were measured for both of the terminal vinyl hydrogens, and an NOE of $-16 \pm 2\%$ was measured for the secondary vinyl hydrogen (Supporting Information Figure 4). Negative NOEs were also observed for the YCH_2 and the *gem*-dimethyl group, although quantification was precluded by the large subtraction errors in the difference spectra.

In contrast, irradiation of the combined Cp* and β-CH_2 resonance of THF adduct **5** (δ 1.88) for 40 ms (0.008 mT) produced an NOE of $<-1\%$ for the terminal vinyl hydrogens and $-2 \pm 1\%$ for the secondary vinyl hydrogen, indicating that the pendant alkene of **5** was not coordinated to the metal center (Supporting Information Figure 5). NOE enhancements of $-12 \pm 2\%$ and $-26 \pm 2\%$ were measured for YCH_2 and for the α-methylene groups of THF, respectively. No NOEs were observed for the *gem*-dimethyl group or for the β-methylene groups of THF, presumably due to subtraction errors in this region of the spectra.

After preliminary 1D NOE experiments were performed, complexes **4** (Figure 1) and **5** (Figure 2) were examined qualitatively by ^{1}H NOESY NMR spectroscopy using a 75 ms mixing time. The magnitude and the distribution of the NOE crosspeaks between the Cp*/β-CH_2 hydrogens and the vinyl hydrogens reveal qualitative information about the structures of **4** and **5**. All of the vinyl hydrogens in **4** show sizable NOEs of nearly equal intensities. The similar intensities imply that all of the vinyl hydrogens are roughly equidistant from the Cp*/β-CH_2 hydrogens, as expected for a coordinated alkene.

In contrast, the spectrum of THF adduct **5** shows a strong NOE between the Cp*/β-CH_2 hydrogens and the α-CH_2 groups of THF but weak NOEs between the Cp*/β-CH_2 hydrogens and the vinyl hydrogens. As expected, the crosspeak between the Cp*/β-CH_2 hydrogens and the secondary vinyl hydrogen is larger than the peak to the two terminal vinyl hydrogens. In further support of these interpretations, the spectra of **4** and **5** exhibit similar crosspeak intensities, correlating the Cp*/β-CH_2 hydrogens to the *gem*-dimethyl and YCH_2 hydrogens.

Quantitative Determination of the Solution Structure of 4 by Conformer Population Analysis. The solution structure of yttrium pentenyl chelate complex **4** was determined by analyzing the time course of the quantitative ^{1}H 2D NOESY data with the multiconformational analysis technique, conformer population analysis (CPA).[20,21]

The 2DCPA method correlates the distance-related information obtained from the buildup of NOE intensities to the NOE data calculated for a large set of energetically feasible model conformations generated by molecular mechanics. The 2DCPA strives to find the smallest combination of conformers that best account for the NOE data. Our approach to analyzing the solution conformations of **4** takes advantage of several distinctive features of the 2DCPA method:[20,21] (1) because the model is multiconformational, one is not forced to describe the structure with a single, averaged conformation; (2) the method employs full-relaxation matrix analysis with accurate simulation of spin-diffusion; (3) all data, including the absence of NOE crosspeaks, are quantitatively analyzed; and (4) the goodness-of-fit is determined by direct comparison of observed data (the time course of NOE intensities) with simulated data. The primary goal of this 2DCPA analysis is to determine whether there is a significant population of the uncoordinated yttrium pentenyl intermediate **A**. A secondary goal is to investigate the detailed geometry of the yttrium−alkene coordination. We note that NOE analysis of the solution structure of these yttrocene complexes presents formidable challenges. By far the greatest challenge is the quantitation and analysis of data arising from 30 chemical shift-equivalent but geometrically inequivalent methyl protons. Only a detailed, quantitative method of analysis, such as 2DCPA, can lead to a reliable interpretation of such data.

(20) (a) Landis, C.; Allured, V. S. *J. Am. Chem. Soc.* **1991**, *113*, 9493. (b) Landis, C. R.; Luck, L.; Wright, J. M. *J. Magn. Reson., Ser. B* **1995**, *109*, 44.

(21) Giovannetti, J. S.; Kelly, C. M.; Landis, C. R. *J. Am. Chem. Soc.* **1993**, *115*, 4040.

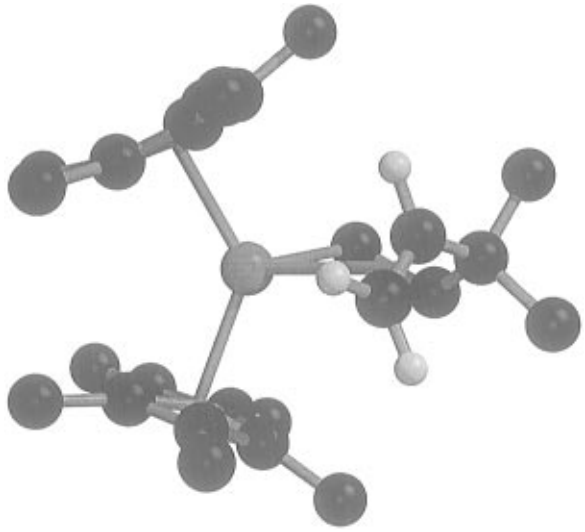

Figure 3. Yttrium pentenyl chelate twist-boat conformer with the lowest single conformation *R*-factor. Its *R*-factor is only slightly higher than that of the chair conformer shown in Figure 4.

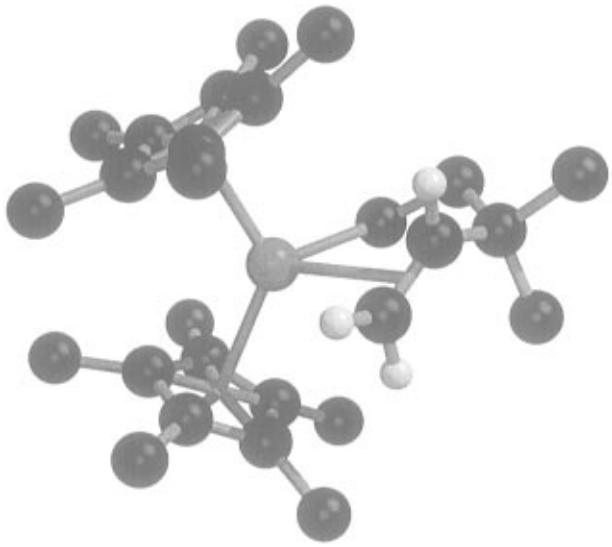

Figure 4. Yttrium pentenyl chelate chair conformer with the lowest single conformation *R*-factor.

There are four steps in our use of the 2DCPA method: (1) quantitation of NOESY time courses, (2) creation of an ensemble of possible solution structures using molecular mechanics methods, (3) quantitative simulation of the complete NOESY time courses for different combinations of structures, and (4) further refinement by dynamics simulations of local motions on the 10 ps time scale.

^{1}H NOESY spectra were obtained at −100 °C at mixing times of 75, 100, 150, and 250 ms. Integration of the diagonal and off-diagonal peaks at all four mixing times and subsequent extrapolation of the diagonal intensities to zero mixing time provided the quantitative time course of NOE buildup.

An initial ensemble of 204 model conformations, 60 conformations for the uncoordinated yttrium pentenyl intermediate **A** and 144 chelate conformations, was generated with CERIUS[2] v1.6 using the universal force field as a starting force field. All modeling used the Qeq charge equilibration method for computing electrostatic interactions. When generating the model conformations for the pentenyl chelate (**4**), nine different force fields were used where the equilibrium distance from Y to the alkene centroid dummy atom (DA) incrementally was set at 2.55, 2.70, and 2.85 Å, and the Y−DA−C5 equilibrium angle incrementally was set at 70, 80, and 90°. These equilibrium values were designed to bracket the 2.70 Å distance and 80° angle found in Zr(IV) oxypentenyl chelate **1**. The free alkene conformations (**A**) in the initial ensemble use a force field corresponding to a monovacant tetrahedral geometry at yttrium.

A second, superset ensemble was generated to test the sensitivity of the initial ensemble to changes in composition. This ensemble included the conformers of the initial set plus conformers generated using eight additional chelate force fields and a free alkene force field corresponding to a trigonal planar geometry at yttrium. The new chelate force fields add a Y−DA equilibrium distance of 3.00 Å, and Y−DA−C5 equilibrium angles of 100 and 110° to the increments described above for a total of 392 conformations.

A number of interesting features of the models of **4** were discovered during the creation of the initial ensemble. The model yttrium pentenyl chelate conformations adopt either a twist-boat or a chair conformation. Examples of each type are shown in Figures 3 and 4. The DA−Y−C1−C2 torsion angles for the chair conformers range from 10° to 38° and from −28° to −36° for the twist-boat conformers. The chair form has a great deal more flexibility, and the chelate ring atoms span a much wider range of positions, especially the *gem*-dimethyl hydrogens. The span of each comformational family can be clearly seen in Figure 5 (see also Supporting Information Figure 6). The twist-boat form is in a narrower, deeper well on the potential energy surface and shows little conformational flexibility.

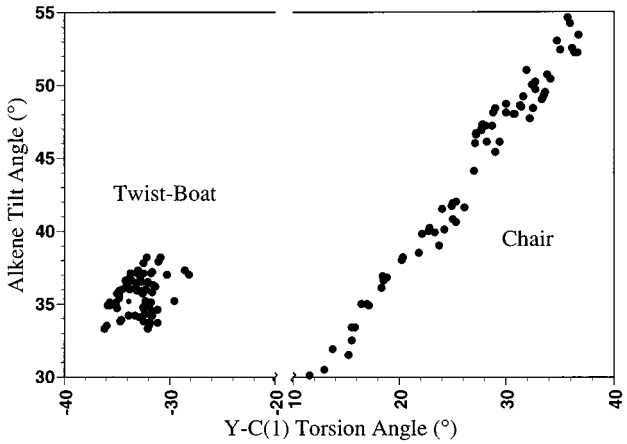

Figure 5. Alkene tilt from the meridional plane *versus* torsion about the yttrium−α carbon bond.

Although it is not possible to directly compare the energies of conformations obtained using different force fields (Supporting Information Figure 7), it is always true that the twist-boat comformers are lower in energy than their chair counterparts by an average of ∼3.5 kcal mol^{-1}. A representative example of the relationship between conformation and energy is shown in Figure 6. The conformers in Figure 6 are members of the initial ensemble found using the force field, with a Y−DA equilibrium bond distance of 2.70 Å and a Y−DA−C5 equilibrium angle of 80°, corresponding to the alkene geometry of **1**.

The inclusion of more than one conformation in NOE analysis will always lead to better agreement between computed and observed spectra. Thus, critical issues for the analysis of the yttrium pentenyl complex **4** are (1) is it significant to use more than one conformation and (2) what is (are) the structure(s) of the conformer(s) that yield(s) the best fit with the fewest significant conformer(s)? We address these issues by comparing the quality of the fit to the NOE data using the best set of one,

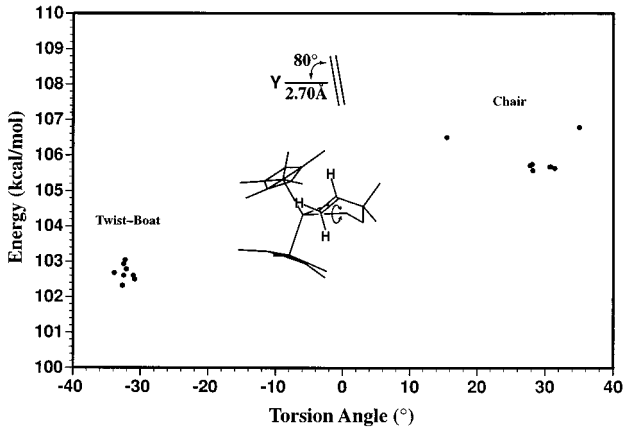

Figure 6. Molecular mechanics energy *versus* the torsion about the yttrium−carbon 1 bond for the force field, with an equilibrium yttrium−dummy atom bond distance of 2.70 Å and yttrium−dummy atom−carbon 5 bond angle of 80°.

two, or three conformers obtained by exhaustive searching of all possible combinations of 392 trial conformations (corresponding to 392, 76 636, and 9 962 680 combinations, respectively).

If the data fitting is limited to a single static conformation, the lowest *R*-factor ($R = 0.336$) is obtained with a chelate structure in the chair conformation. This conformation, which is illustrated in Figure 4, exhibits asymmetric $Y-C_{alkene}$ distances (2.42 and 2.86 Å), with the shorter bond occurring between the Y and the terminal alkene carbon. This asymmetry is not significant, however, because the next best fitting conformer is a twist-boat structure with symmetric $Y-C_{alkene}$ distances (2.93 Å) and a very similar *R*-factor ($R = 0.339$).

The best fit to a set of two conformers ($R = 0.301$) is a 70:30 ratio of a twist-boat chelate conformer:unchelated conformer. The best set of three conformers ($R = 0.300$) is a 58:29:13 ratio of a twist-boat conformer : an unchelated conformer : a chair conformer. Application of the *F*-test at the 95% confidence level indicates that it is statistically significant to use two rather than one conformation in fitting the data but that three conformations do not lead to a significantly better fit relative to two conformations. In general, we find that the *R*-factor for the fitting of the data is not particularly sensitive to the details of the alkene coordination geometry. It is not possible, with this data, to distinguish between symmetric vs asymmetric alkene coordination modes or to define a precise (i.e., at higher resolution than ca. 0.4 Å) metal−alkene centroid distance.

Flexible molecules such as **4** undergo local motion that is rapid compared with the time scale of molecular tumbling (ca. 1 ns). Previously reported applications of 2DCPA have been limited to consideration of static structures.[20,21] In order to develop the physically most realistic model of the NOE experiment, we have implemented a feature in the 2DCPA program that accounts for rapid motion by calculating NOE intensities averaged in r^{-3} space. This refinement step takes the static structures which led to the best fit of the data and simulates their local fluctuations by running short molecular dynamics trajectories. This approach is efficient because it only requires computing trajectories for a small number of starting conformations that possess the structural features that best fit the observed NMR data.

Eighteen conformations were selected on the basis of contribution to a best-of-class (with respect to force field) fit to the observed data either singly or in combination with another conformer in a doubles solution. Most of the best singles are common denominators in best-of-class two conformer fits. The resulting ensemble contains five chair, 11 twist-boat, and two free structures averaged over 10 ps at 220 K. An *R*-factor of 0.318 was obtained for the single best fit averaged conformation, which is a chelate structure in the chair conformation. This conformation has Y−C5 and Y−C4 distances of 3.02 and 2.58 Å, respectively. Two-conformer dynamic fitting yields an *R*-factor of 0.308 for a structure that is 53% twist-boat and 47% chair chelate conformation. The *F*-test results for the dynamically averaged fitting indicate that, at most, two conformers are statistically significant with 95% confidence. As found for the static fitting, we cannot distinguish details of the alkene coordination geometry, such as asymmetry or precise metal−alkene centroid distances, only on the basis of the NOE data.

Scheme 3

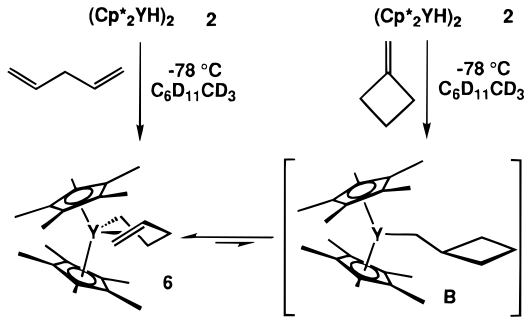

Synthesis of Pentenyl Chelate Complex $Cp^*_2Y[\eta^1,\eta^2\text{-}CH_2CH_2CH_2CH{=}CH_2]$ (6). To test whether chelation requires promotion by a *gem*-dimethyl group, yttrium hydride dimer **2** was reacted with 1,4-pentadiene in methylcyclohexane-d_{14} at −78 °C. A bright yellow solution of the thermally unstable pentenyl chelate complex $Cp^*_2Y[\eta^1,\eta^2\text{-}CH_2CH_2CH_2CH{=}CH_2]$ (**6**) was formed in 85 ± 5% yield (^{1}H NMR spectroscopy, $CH_2(SiMe_3)_2$ internal standard) (Scheme 3). **6** was characterized by ^{1}H and ^{13}C NMR spectroscopy at −100 °C. Formation of **6** demonstrates that the *gem*-dimethyl group on the pentenyl backbone is not required to form a stable alkene chelate. Addition of H_2 to a solution of **6** resulted in hydrogenation of the pentenyl chain to give pentane, which was identified by ^{1}H NMR spectroscopy and GC/MS analysis.

The ^{1}H and ^{13}C NMR chemical shifts for **6** closely resemble the shifts observed for chelate complex **4**. In the ^{1}H NMR spectrum, evidence for alkene coordination is seen in the large difference in chemical shift of the terminal vinyl hydrogens (δ 3.79, d, $J_{cis} = 10.0$ Hz; 5.25, d, $J_{trans} = 17.5$ Hz; $\Delta\delta = 1.46$ ppm) and in the 1 ppm shift to higher frequency of the secondary vinyl hydrogen (δ 6.58, m) (Table 1, Supporting Information Figure 8). A single resonance at δ 1.91 was observed for the Cp* ligands, indicating that **6** is rapidly fluxional.

In the ^{13}C NMR spectrum of **6**, the resonance for the terminal alkene carbon (δ 112.9) is shifted 3 ppm to lower frequency than in 1,4-pentadiene, and the resonance for the internal vinyl carbon (δ 158.1) is shifted 22 ppm to higher frequency (Table 1). Methylene resonances were observed at δ 14.7 (YCH_2CH_2), 33.7 (d, $J_{YC} = 44.8$ Hz, YCH_2), and 39.4 ($YCH_2CH_2CH_2$). Resonances at δ 11.6 and 116.3 were assigned to the Cp* methyl and Cp* ring carbon atoms, respectively.

Pentenyl chelate **6** was also generated from the reaction of yttrium hydride dimer **2** and methylenecyclobutane at −78 °C, presumably via the methylcyclobutyl intermediate **B** (Scheme 3). **6** was formed in 98 ± 5% yield from **2** and methylenecyclobutane (^{1}H NMR spectroscopy, $CH_2(SiMe_3)_2$ internal standard) (Supporting Information Figure 9). Formation of **6** from **2** and methylenecyclobutane demonstrates that ring-opening via β-alkyl elimination is facile and that the pentenyl chelate complex is favored over the methylcyclobutyl derivative.

Scheme 4

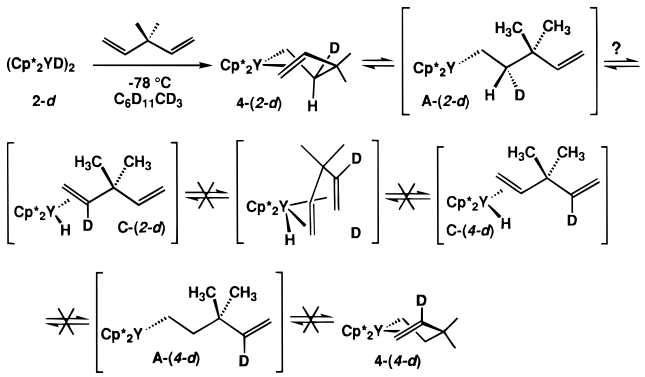

When the reaction of yttrium hydride dimer **2** and methylenecyclobutane was analyzed by ^{1}H NMR spectroscopy 10 min after the reagents were mixed at −78 °C, pentenyl chelate **6** was the only yttrium compound observed in solution. The failure to observe presumed methylcyclobutyl intermediate **B** implies a half-life for conversion to **6** of ≤2 min at −78 °C ($\Delta G^{\ddagger} \leq 13.2$ kcal mol^{-1}).

The interconversion of methylcyclobutyl and pentenyl ligands has been observed in several similar systems.[22−25] Silver ion abstraction of Cl^- from the methylcyclobutylplatinum complex $(PMe_3)_2ClPtCH_2C(CH_3)CH_2CH_2CH_2$ at −78 °C resulted in rapid ring-opening to give the platinum pentenyl chelate complex $[(PMe_3)_2Pt(\eta^1,\eta^2\text{-}CH_2CH_2CH_2C(CH_3){=}CH_2)]^+$.[23a] Marks has studied the cationic zirconocene-catalyzed ring-opening polymerization of methylenecyclobutane and observed that ring-opening is more facile than monomer insertion.[25]

Reaction of (Cp*$_2$YD)$_2$ (2-*d*) and 3,3-Dimethyl-1,4-pentadiene. The reversibility of yttrium hydride addition was investigated by studying the reaction of the yttrium deuteride dimer $(Cp^*_2YD)_2$ (**2**-*d*) with 3,3-dimethyl-1,4-pentadiene. This reaction cleanly produced the monodeuterated yttrium pentenyl chelate complex $Cp^*_2Y[\eta^1,\eta^2\text{-}CH_2CHDC(CH_3)_2CH{=}CH_2]$ (**4**-(**2**-*d*)) in 88 ± 5% yield (^{1}H NMR spectroscopy, $CH_2(SiMe_3)_2$ internal standard). Deuterium scrambling might have occurred by the sequence outlined in Scheme 4: β-Hydrogen elimination from **4**-(**2**-*d*) would give the yttrium−hydride−η^2-alkene intermediate **C**-(**2**-*d*); interchange of complexed alkenes might occur through the bis-η^2-alkene intermediate **D**; readdition of hydride could form the deuterium scrambled chelate complex $Cp^*_2Y[\eta^1,\eta^2\text{-}CH_2CH_2C(CH_3)_2CD{=}CH_2]$ (**4**-(**4**-*d*)). Formation of **4**-(**4**-*d*) would result in a change in the relative intensities and coupling constants of the vinyl protons. Complex **4**-(**2**-*d*) was monitored by ^{1}H NMR spectroscopy at −78 °C, and no deuterium scrambling was detected after 90 h. This indicates that reversible β-hydrogen elimination in conjunction with alkene interchange via bis-η^2-alkene intermediate **D** is slow. The lack of deuterium scrambling is in accord with Bercaw's observation that Cp^*_2Sc−alkyl compounds do not undergo β-hydride elimination below 0 °C.[26]

Reaction of 2 and 1,4-Pentadiene-1,1,5,5-*d*$_4$. Generation of pentenyl chelate **6** from **2** and methylenecyclobutane was consistent with the facile conversion of the yttrium methylcyclobutyl intermediate **B** to pentenyl chelate complex **6** at −78 °C. A deuterium labeling study was performed to determine if **B** was kinetically accessible from **6** under the reaction conditions. Reaction of yttrium hydride dimer **2** with 1,4-pentadiene-1,1,5,5-d_4 should generate the tetradeuterated pentenyl chelate complex $Cp^*_2Y[\eta^1,\eta^2\text{-}CD_2CH_2CH_2CH{=}CD_2]$ **6**-1,1,5,5-d_4 (Scheme 5). Intramolecular alkene insertion into the Y−C bond to form the methylcyclobutyl intermediate **B**-d_4 followed by ring-opening β-alkyl elimination would form both **6**-1,1,5,5-d_4 and $Cp^*_2Y[\eta^1,\eta^2\text{-}CH_2CH_2CD_2CH{=}CD_2]$ (**6**-3,3,5,5-d_4).

Addition of 1,4-pentadiene-1,1,5,5-d_4 to a solution of yttrium hydride **2** at −78 °C formed a mixture of pentenyl chelate complexes **6**-1,1,5,5-d_4 and **6**-3,3,5,5-d_4 which was initially enriched in the **6**-1,1,5,5-d_4 isotopomer. The initial ^{1}H NMR spectrum (∼10 min) displayed a very weak and broad resonance at δ 0.40, corresponding to the YCH_2 resonance of **6**-3,3,5,5-d_4. This resonance gradually increased in intensity over 2 h. However, due to the overlap of the broad YCH_2 resonance with the resonance for the internal standard [δ 0.25, $CH_2(SiMe_3)_2$], the kinetics for the interconversion could not be accurately determined by ^{1}H NMR spectroscopy. In the ^{13}C NMR spectrum taken at −78 °C after 20 h, the observation of a γ-CH_2 resonance at δ 39.1 and a γ-CD_2 resonance at δ 38.4 ($\omega_{1/2}$ = 32 Hz, isotope shift = 72 ppb) confirmed the presence of both **6**-1,1,5,5-d_4 and **6**-3,3,5,5-d_4 in solution (Supporting Information Figure 10).

The rate of approach to equilibrium of chelate complex **6**-1,1,5,5-d_4 and **6**-3,3,5,5-d_4 was determined by periodic hydrogenolysis of **6**, which generated **2**, pentane-1,1,5,5-d_4, and pentane-3,3,5,5-d_4 (Scheme 5). The ratio of pentane isotopomers was determined by both ^{2}H NMR spectroscopy and analysis of the GC/MS fragmentation ratios.

In the ^{2}H NMR spectrum, resonances were observed at δ 1.13 for the CD_2 unit of pentane-3,3,5,5-d_4 and at δ 0.84 for the two CHD_2 units of pentane-1,1,5,5-d_4 and the single CHD_2 unit of pentane-3,3,5,5-d_4 (Table 2). Assuming that an equilibrium 1:1 mixture of **6**-1,1,5,5-d_4:**6**-3,3,5,5-d_4 would produce a 3:1 ratio of CHD_2 to CD_2 resonances, the percentage of **6**-1,1,5,5-d_4 in excess of the equilibrium value was derived from the relative ratio of the two resonances. A linear plot of ln [% excess **6**-1,1,5,5-d_4] versus time established a first-order rate law for the approach to equilibrium for the conversion of **6**-1,1,5,5-d_4 to **6**-3,3,5,5-d_4 (Supporting Information Figure 11): rate = k_1[**6**-1,1,5,5-d_4], where $k_1 = (3.9 \pm 0.7) \times 10^{-4}$ s^{-1} ($\Delta G^{\ddagger} = 14.3 \pm 0.1$ kcal mol^{-1}) at −78 °C, which corresponds to a half-life of 30 min.

Similarly, the percent excess of **6**-1,1,5,5-d_4 was independently determined from the ratio of the $(C_3H_5D_2)^+$ and $(C_3H_3D_4)^+$ propyl fragments in the mass spectra of mixtures of pentane-1,1,5,5-d_4 and pentane-3,3,5,5-d_4 (Table 3). Using analogous data treatment this analysis provided the first-order rate constant of $k_1 = (2.8 \pm 0.3) \times 10^{-4}$ s^{-1} ($\Delta G^{\ddagger} = 14.4 \pm 0.1$ kcal mol^{-1}) at −78°C (Supporting Information Figure 11) which corresponds to a half-life of 40 min, in reasonable agreement with the first-order rate constant obtained from ^{2}H NMR analysis.

An energy diagram for pentenyl chelate **6**, methylcyclobutyl intermediate **B**, and η^1-intermediate **E** was constructed using these kinetic data (Figure 7). The rate of deuterium scrambling between **6**-1,1,5,5-d_4 and **6**-3,3,5,5-d_4 established a barrier of 14.4 ± 0.2 kcal mol^{-1} for intramolecular alkene insertion into pentenyl chelate complex **6**. Although the interconversion of deuterium-labeled chelates **6**-1,1,5,5-d_4 and **6**-3,3,5,5-d_4 con-

(22) Bunel, E.; Burger, B. J.; Bercaw, J. E. *J. Am. Chem. Soc.* **1988**, *110*, 976.

(23) (a) Flood, T. C.; Statler, J. A. *Organometallics* **1984**, *3*, 1795. (b) Flood, T. C.; Bitler, S. P. *J. Am. Chem. Soc.* **1984**, *106*, 6076. (c) Ermer, S. P.; Struck. G. E.; Bitler, S. P.; Richards, R.; Bau, R.; Flood, T. C. *Organometallics* **1993**, *12*, 2634.

(24) Golden, H. J.; Baker, D. J.; Miller, R. G. *J. Am. Chem. Soc.* **1974**, *96*, 4235.

(25) (a) Yang, X.; Jia, L.; Marks, T. J. *J. Am. Chem. Soc.* **1993**, *115*, 3392. (b) Jia, L.; Yang, X.; Seyam, A. M.; Albert, I. D. L.; Fu, P.-F.; Yang, S.; Marks, T. J. *J. Am. Chem. Soc.* **1996**, *118*, 7900.

(26) (a) Parkin, G.; Bunel, E.; Burger, B. J.; Trimmer, M. S.; Asselt, A. V.; Bercaw, J. E. *J. Mol. Catal.* **1987**, *41*, 21. (b) Burger, B. J.; Thompson, M. E.; Cotter, W. D.; Bercaw, J. E. *J. Am. Chem. Soc.* **1990**, *112*, 1566.

Scheme 5

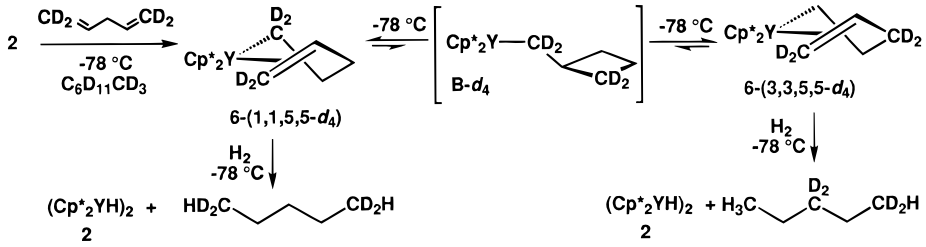

Table 2. $^2H\{^1H\}$ NMR Analysis of a Mixture of Pentane-1,1,5,5-d_4 and Pentane-3,3,5,5-d_4 Obtained from Addition of H_2 to a Solution of **6**-1,1,5,5-d_4 and **6**-3,3,5,5-d_4

time of H_2 addition (min)	% δ 0.84 (CHD_2)	% δ 1.13 (CD_2)	% excess **6**-1,1,5,5-d_4
0	94.7	5.3	79
15	91.6	8.4	66
30	88.5	11.5	54
60	80.0	20.0	20
1440	73.0	27.0	−8

Table 3. MS Analysis of a Mixture of Pentane-1,1,5,5-d_4 and Pentane-3,3,5,5-d_4 Obtained from Addition of H_2 to a Solution of **6**-1,1,5,5-d_4 and **6**-3,3,5,5-d_4

time of H_2 addition (min)	% $m/e = 45$, $(C_3H_5D_2)^+$	% $m/e = 47$, $(C_3H_3D_4)^+$	% excess **6**-1,1,5,5-d_4
0	93.8	6.2	75
15	91.6	8.4	66
30	87.7	12.3	51
60	81.9	18.1	28
1440	76.9	23.1	8

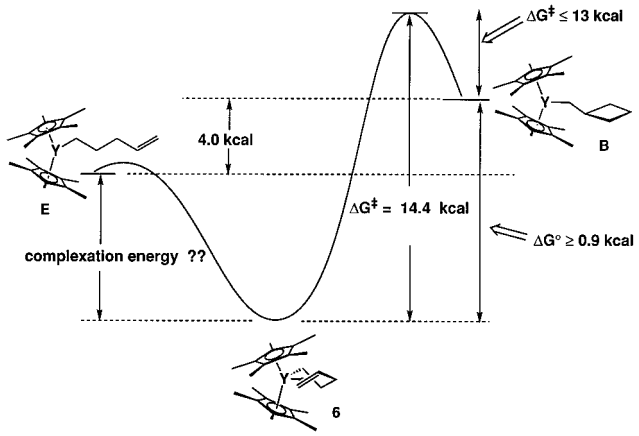

Figure 7. Energy diagram for pentenyl chelate **6**, methylcyclobutyl intermediate **B**, and η^1-pentenyl intermediate **E**.

firmed the presence of an equilibrium between **6** and methylcyclobutyl intermediate **B**, the energy difference between **6** and **B** is not well defined. Assuming that 5% of **B** would have been detected by ^1H NMR spectroscopy, a lower limit for the equilibrium constant of ≥ 20 ($\Delta G° \geq 0.9$ kcal mol^{-1}) can be estimated. The rate of formation of **6** from **2** and methylenecyclobutane establishes that the barrier for ring-opening in intermediate **B** to form chelate **6** must be ≤ 13 kcal mol^{-1}. Assuming equivalent Y−C bond strengths, methylcyclobutyl intermediate **B** was calculated to be 4.0 kcal mol^{-1} less stable than unchelated yttrium η^1-pentenyl intermediate **E** using Benson's additivity rules.[27]

(27) Benson, S. W. *Thermochemical Kinetics*; Wiley: New York, 1968.

Discussion

Intramolecular Alkene Coordination in Yttrium(III) Pentenyl Chelate Complex 4. The ^1H and ^{13}C NMR chemical shifts for the coordinated alkene of yttrium pentenyl chelate complex **4** suggest that the double bond is unsymmetrically bound to the d⁰ yttrium metal center. In particular, the secondary vinyl hydrogen atom (δ 6.78) is shifted 1 ppm to higher frequency in the ^1H NMR spectrum, and the internal vinyl carbon atom (δ 161.1) is shifted 15 ppm to higher frequency in the ^{13}C NMR spectrum relative to 1,4-pentadiene, which suggests that the internal alkene carbon atom is positively polarized. This partial positive charge may help to explain the rapid rate of addition of the alkyl metal unit to the carbon-carbon double bond.

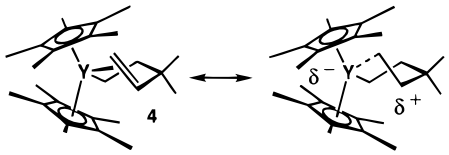

Yttrium pentenyl chelate complex **6** (δ 6.58, =C*H*; 158.1, =*C*H) and zirconium(IV) oxypentenyl chelate complex **1** (δ 7.51, =C*H*; 159.2, =*C*H) display similar NMR resonances for complexation of a pendant alkene to a d⁰ metal center. Asymmetric bonding in chelate complex **1** was confirmed by X-ray crystallography, which showed that the terminal alkene carbon atom was 0.21 Å closer to Zr than the internal alkene carbon atom (Zr−C4 = 2.89 Å; Zr−C5 = 2.68 Å).

Mulliken population analysis of the RHF wavefunction of the hypothetical cationic titanium(IV) methyl ethylene complex $CH_3TiCl_2(C_2H_4)^+$ shows a highly polarized ethylene ligand and significant charge transfer from the coordinated alkene to the d⁰ metal center.[28] Nonlocal DFT calculations of the cationic zirconium(IV) methyl ethylene complex $H_2SiCp_2ZrCH_3$-$(CH_2{=}CH_2)^+$ indicate that ethylene is strongly polarized and asymmetrically bonded to the d⁰ metal center.[29] The distance from the alkene carbon atoms to Zr differs by 0.24 Å (2.65 Å; 2.89 Å).

Analysis of low-temperature NOE data for the yttrium pentenyl chelate complex **4** supports the chelate conformation. Exhaustive searches of an ensemble of 392 conformations at the one, two, and three conformer levels yield a subset of the best fitting static conformations for one and two conformer solutions. Averaging short dynamics trajectories of this subset in r^{-3} space gives an 18-conformer ensemble that best fits the observed data when taken as an approximately equal mixture (53:47) of twist-boat and chair chelated conformations. At least as judged by the *F*-test at the 95% confidence level, the use of two conformations vs one conformation is justified. The data do not reveal the intimate details of the yttrium−alkene

(28) Kawamura-Kuribayashi, H.; Koga, N.; Morokuma, K. *J. Am. Chem. Soc.* **1992**, *114*, 2359.

(29) Yoshida, N.; Koga, N.; Morokuma, K. *Organometallics* **1995**, *14*, 746 and references therein.

coordination, such as the extent of asymmetry or the precise metal−alkene centroid distances.

Fluxionality of Chelate Complexes 4 and 6. The observation of equivalent Cp* and *gem*-dimethyl groups for pentenyl chelate complex **4** at −100 °C suggests that a rapid fluxional process is occurring involving dissociation and recoordination of the chelated alkene. The facile equilibration of the diastereotopic groups is consistent with the expected weakness of an interaction between an alkene and a group III or neutral group IV metal center.[4] An upper limit of 10.4 kcal mol^{-1} for the intramolecular alkene binding energy in the yttrium(III) pentenyl chelate complexes can be estimated on the basis of the 14.4 ± 0.1 kcal mol^{-1} barrier for the conversion of pentenyl chelate complex **6** to methylcyclobutyl intermediate **B** and the 4.0 kcal mol^{-1} energy difference between **B** and the yttrium(III) η^1-pentenyl intermediate **E** (Figure 7).

Interaction between an alkene and a cationic group IV metal center is expected to be stronger due to a charge-induced dipole interaction.[30] This is consistent with the observation of a barrier of $\Delta G^{\ddagger} = 10.7 \pm 0.1$ kcal mol^{-1} for the interconversion of the Cp ligands of zirconium(IV) oxypentenyl chelate complex **1**. Equilibration of the Cp ligands in **1** can occur by either dissociation of the coordinated alkene or displacement of the alkene by CD_2Cl_2 or $MeB(C_6F_5)_3^-$ followed by recoordination of the opposite face of the alkene.

Conclusion

We have demonstrated that stable d^0 transition metal−alkyl−alkene complexes can be generated from the reaction of yttrium hydride **2** with 1,4-pentadiene derivatives and with methylenecyclobutane. These yttrium(III) pentenyl chelate complexes serve as excellent models for the proposed d^0 metal−alkyl−alkene intermediate in Ziegler−Natta polymerization reactions. The rapid equilibration of the diastereotopic Cp* and Me groups of chelate complex **4** at −100 °C is consistent with the expected weakness of the d^0 metal−alkene interaction, and the characterization of **4** by ^{1}H and ^{13}C NMR spectroscopy suggests that the internal alkene carbon atom is positively polarized. The interconversion of deuterium-labeled chelate complexes **6**-1,1,5,5-d_4 and **6**-3,3,5,5-d_4 establishes that intramolecular alkene insertion occurs reversibly at −78 °C.

Experimental Section

General Methods. All manipulations were performed under a nitrogen atmosphere in an inert atmosphere glovebox or by standard high-vacuum techniques. All reactions were performed in 1.9 mL medium-walled resealable NMR tubes. 500 MHz ^{1}H NMR spectra, 126 MHz ^{13}C{^{1}H} NMR spectra, and 76 MHz ^{2}H{^{1}H} NMR spectra were obtained on a Bruker AM500 spectrometer. 91 MHz ^{13}C NMR spectra were obtained on a Bruker AM360 spectrometer. Solvent-obscured methylene resonances in the ^{13}C NMR spectra of **4**−**6** were assigned by DEPT-135 experiments. 1D NOE and ^{1}H NOESY NMR spectra were obtained on a Varian Unity 500 with a 5 mm ^{1}H/^{19}F probe. Probe temperatures were calibrated with a methanol standard. Mass spectra were determined on a Kratos MS-25 spectrometer attached to a Carlo Erba gas chromatograph equipped with a 60 m DB-5 column.

1,4-Pentadiene-1,1,5,5-d_4[31] and Cp*$_2$YCH(SiMe$_3$)$_2$ (**3**)[13] were prepared by known procedures. Methylcyclohexane-d_{14} (Cambridge Isotopes), toluene-d_8 (Cambridge Isotopes), 3,3-dimethyl-1,4-pentadiene (Wiley Organics), toluene, and THF were distilled from sodium/potassium alloy. 1,4-Pentadiene (Aldrich) and 1,4-pentadiene-1,1,5,5-d_4 were distilled from $NaBH_4$, and methylenecyclobutane (Aldrich) was distilled from sodium. H_2 (Liquid Carbonic) was used as received.

General Procedure for Preparation of (Cp*$_2$YH)$_2$ (2).[13] An NMR tube containing Cp*$_2$YCH(SiMe$_3$)$_2$ (**3**)[13] (11−18 mg, 0.021−0.035 mmol) in 0.30−0.40 mL of methylcyclohexane-d_{14} was sealed under 1 atm of H_2 at 77 K and warmed to 0 °C (H_2 pressure at 0 °C is calculated to be ≤3.5 atm). After shaking of the tube periodically for 15 min, H_2 was removed via three freeze−pump−thaw cycles to give (Cp*$_2$YH)$_2$ (**2**) and $CH_2(SiMe_3)_2$ in 95−100% yield by ^{1}H NMR spectroscopy. **2** was freshly prepared prior to each reaction and was used without isolation. $CH_2(SiMe_3)_2$ served as an internal standard for subsequent reactions. ^{1}H NMR (500 MHz, $C_6D_{11}CD_3$, −100 °C): in addition to resonances corresponding to $CH_2(SiMe_3)_2$ at δ −0.25 and 0.03, resonances were observed at δ 2.07 (s, C_5Me_5) and 5.32 (t, J_{YH} = 37.5 Hz, Y-H). ^{13}C{^{1}H} NMR (126 MHz, $C_6D_{11}CD_3$, −100 °C): in addition to resonances corresponding to $CH_2(SiMe_3)_2$ at δ 1.34 and 3.84, resonances were observed at δ 12.4 (s, $C_5\mathit{Me}_5$) and 118.6 (s, C_5Me_5).

(Cp*$_2$YD)$_2$ (2-*d*). Reaction of **3** and D_2 employing a procedure analogous to that used to synthesize **2** generated **2**-*d* in 99 ± 5% by yield ^{1}H NMR spectroscopy. ^{1}H NMR (500 MHz, $C_6D_{11}CD_3$, −100 °C): in addition to resonances corresponding to $CHD(SiMe_3)_2$ (δ −0.30, 1 H; 0.03, 18 H), a single resonance was observed at δ 2.07 (s, C_5Me_5).

Cp*$_2$Y[η^1,η^2-CH$_2$CH$_2$C(CH$_3$)$_2$CH=CH$_2$] (4). 2 was prepared in *situ* by hydrogenation of a solution of **3** (11.4 mg, 0.022 mmol) in 0.32 mL of methylcyclohexane-d_{14}. 3,3-Dimethyl-1,4-pentadiene (0.024 mmol) was vacuum transferred into the NMR tube, which was sealed and shaken once at −78 °C to produce a bright yellow solution of **4** (98 ± 5% yield by ^{1}H NMR spectroscopy using $CH_2(SiMe_3)_2$ as an internal standard vs Cp* resonance). **4** was also prepared in toluene-d_8 in 84 ± 5% NMR yield. **4** was thermally unstable and was analyzed without isolation by ^{1}H and ^{13}C NMR spectroscopy at −100 °C. ^{1}H NMR (500 MHz, $C_6D_{11}CD_3$, −100 °C): δ −0.44 (br s, $\omega_{1/2}$ = 24 Hz, YCH_2), 1.03 (s, CH_3), 1.82 (br s, $\omega_{1/2}$ = 12 Hz, $YCH_2C\mathit{H}_2$), 1.93 (s, C_5Me_5), 3.76 (d, J_{cis} = 10.7 Hz, =C*H*H), 5.14 (d, J_{trans} = 17.8 Hz, =CH*H*), 6.78 (dd, J = 17.8, 10.7 Hz, CH=). ^{1}H NMR (500 MHz, $C_6D_{11}CD_3$, −50 °C): δ −0.41 (br s, $\omega_{1/2}$ = 22 Hz, YCH_2), 1.03 (s, CH_3), 1.82 (s, $YCH_2C\mathit{H}_2$), 1.93 (s, C_5Me_5), 3.83 (d, J_{cis} = 10.7 Hz, =C*H*H), 5.13 (d, J_{trans} = 17.8 Hz, =CH*H*), 6.76 (dd, J = 17.8, 10.7 Hz, CH=). ^{1}H NMR (500 MHz, $C_6D_5CD_3$, −80 °C): δ −0.10 (br s, YCH_2), 1.09 (s, CH_3), 1.80 (s, $YCH_2C\mathit{H}_2$), 1.92 (s, C_5Me_5), 3.50 (d, J_{cis} = 9.0 Hz, =C*H*H), 4.90 (d, J_{trans} = 17.5 Hz, =CH*H*), 6.70 (dd, J = 17.5, 9.0 Hz, CH=). ^{13}C{^{1}H} NMR (126 MHz, $C_6D_{11}CD_3$, −100 °C): δ 11.6 (s, $C_5\mathit{Me}_5$), 14.6 (s, $YCH_2\mathit{C}H_2$), 33.7 (d, J_{YC} = 45.8 Hz, YCH_2), 41.2 (s, $\mathit{C}Me_2$), 43.1 (s, CMe_2), 110.5 (s, =CH_2), 116.3 (s, C_5Me_5), 161.1 (s, CH=). ^{13}C NMR (91 MHz, $C_6D_{11}CD_3$, −100 °C): δ 11.6 (q, J_{CH} = 126 Hz, $C_5\mathit{Me}_5$), 41.2 (s, $\mathit{C}Me_2$), 43.1 (q, J_{CH} = 126 ± 2 Hz, CMe_2), 110.5 (t, J_{CH} = 154 ± 2 Hz, =CH_2), 116.3 (s, C_5Me_5), 161.1 (d, J_{CH} = 151 ± 2 Hz, CH=), the $YCH_2C\mathit{H}_2$ resonance was not resolved, and the YCH_2 resonance was obscured by residual solvent peaks. ^{13}C{^{1}H} NMR (126 MHz, $C_6D_5CD_3$, −80 °C): δ 11.8 (s, $C_5\mathit{Me}_5$), 14.9 (s, $YCH_2\mathit{C}H_2$), 33.6 (d, J_{YC} = 44.6 Hz, YCH_2), 41.2 (s, $\mathit{C}Me_2$), 43.3 (s, CMe_2), 111.3 (s, =CH_2), 116.6 (s, C_5Me_5), 160.2 (s, CH=).

Hydrogenation of 4. **2** was prepared *in situ* by hydrogenation of a solution of **3** (14.0 mg, 0.027 mmol) in 0.30 mL of methylcyclohexane-d_{14}. 3,3-Dimethyl-1,4-pentadiene (0.057 mmol) was vacuum transferred into the NMR tube, which was sealed under 1 atm of H_2 (0.289 mmol) at 77 K. The bright yellow solution was shaken periodically at −78 °C for 15 min and then warmed to room temperature to form a pink solution. Unreacted H_2 was removed via three freeze−pump−thaw cycles, and the mixture was analyzed by ^{1}H and ^{13}C NMR spectroscopy. 3,3-Dimethylpentane was formed in 101 ± 5% yield by ^{1}H NMR spectroscopy using $CH_2(SiMe_3)_2$ as an internal standard (CMe_2 resonance vs $SiMe_3$). The solution also contained **2** (48 ± 5%) (Cp* resonance vs $SiMe_3$) and numerous Cp*-containing decomposition products. The ^{1}H NMR[32] and ^{13}C NMR[33] spectra of 3,3-dimethylpentane were consistent with published values.

In a similar experiment, volatile material was vacuum transferred and analyzed by low-resolution GC/MS. 3,3-Dimethylpentane was detected by GC/MS(EI): found for C_7H_{16} [*m*/*e* (intensity)], [M − 15]$^+$

(30) Jensen, V. R.; Siegbahn, P. E. M. *Chem. Phys. Lett.* **1993**, *212*, 353 and references therein.

(31) Yasuda, H.; Ohnuma, Y.; Nakamura, A.; Kai, Y.; Yasuoka, N.; Kasai, N. *Bull. Chem. Soc. Jpn.* **1980**, *53*, 1101.

(32) Whalon, M. R.; Grady, G. L.; McGoff, P.; Domingue, R. P.; Bushweller, C. H. *Tetrahedron Lett.* **1982**, *23*, 5247.

(33) Beierbeck, H.; Saunders, J. K. *Can. J. Chem.* **1977**, *55*, 771.

85 (16), $[M - 29]^+$ 71 (60), $[M - 57]^+$ 43 (100), toluene ($m/z = 92$), and $CH_2(SiMe_3)_2$ ($m/z = 160$). The mass spectra of 3,3-dimethylpentane[34] and $CH_2(SiMe_3)_2$[35] were consistent with published data.

$Cp^*_2Y[\eta^1$-$CH_2CH_2C(CH_3)_2CH{=}CH_2](THF)$ (5). 2 was prepared *in situ* by hydrogenation of a solution of **3** (11.4 mg, 0.022 mmol) in 0.32 mL of methylcyclohexane-d_{14}. 3,3-Dimethyl-1,4-pentadiene (0.022 mmol) was vacuum transferred into the NMR tube, which was sealed and shaken once at −78 °C to form a bright yellow solution of **4**. THF (0.029 mmol) was then vacuum transferred into the tube, which was sealed and shaken once at −78 °C to produce a colorless solution of $Cp^*_2Y[\eta^1$-$CH_2CH_2C(CH_3)_2CH{=}CH_2](THF)$ (**5**) (97 ± 5% yield by ^1H NMR spectroscopy using $CH_2(SiMe_3)_2$ as an internal standard vs Cp*). **5** was thermally unstable and was analyzed without isolation by ^1H and ^{13}C NMR spectroscopy at −100 °C. ^1H NMR (500 MHz, $C_6D_{11}CD_3$, −100 °C): δ −0.74 (br s, YCH_2), 0.90 (s, CH_3), 1.35 (br m, β-THF), 1.88 (s, C_5Me_5), 3.64 (br s, α-THF), 4.75 (m, $=CH_2$), 5.78 (dd, $J = 17.8$, 10.9 Hz, CH=), resonance for $YCH_2CH_2CH_2$ obscured by resonance for Cp* ligands. $^{13}C\{^1H\}$ NMR (126 MHz, $C_6D_{11}CD_3$, −100 °C): δ 11.6 (s, C_5Me_5), 14.7 (s, YCH_2CH_2), 25.7 (s, β-THF), 33.7 (d, $J_{YC} = 50.3$ Hz, YCH_2), 39.6 (s, CMe_2), 43.5 (s, CMe_2), 67.7 (s, α-THF), 108.4 (s, $=CH_2$), 115.2 (s, C_5Me_5), 150.7 (s, CH=).

Collection of ^1H NOESY NMR Data for CPA Analysis. Spectra of 0.050 M solutions of both **4** and **5** were obtained at −100 °C in methylcyclohexane-d_{14}. Spectra were gathered at 75, 100, 150, and 250 ms mixing times using a phase-sensitive NOESY pulse sequence with an initial homospoil pulse and States−Haberkorn−Ruben phase cycling.[36] A 10% random variation in mixing times was used to suppress COSY contamination. Data sets with t_1 and t_2 dimensions of 800 (400 increments) and 1024 complex points, respectively, were collected with relaxation delays of 4.5 s for eight scans of each FID. The FELIX NMR software package from Molecular Simulations, Inc. was used to transform and process the data. t_1 was zero-filled to 1024 points, and t_2 was zero-filled to 2048 points. A linear prediction scheme was used to correct the first point of each FID. Linear prediction was also applied at the tail of each FID and interferogram, extending the data by one-third. A Kaiser window function was applied to the tails in F_1 and F_2 to reduce apodization artifacts, effectively removing most of the tail linear prediction while preserving the acquired data. Low-order polynomial baseline corrections were applied to F_2. Following final phase correction in each dimension, the baselines were corrected using FACELIFT from the National Magnetic Resonance Facility at Madison. Diagonal peak volumes at zero mixing times were estimated by fitting the observed diagonal peaks to an exponential function. For off-diagonal peaks, the intensities of the two symmetry related peaks were averaged prior to normalization.

Generation of Model Conformers. All of the model conformers were generated with CERIUS^2 v1.6 from Molecular Simulations, Inc. using the universal force field as the default force field. In all cases, charges were turned on and equilibrated every 100 steps during dynamics and every 50 steps during minimization using Qeq Charged v1.1. Four independent starting conformers were created by sketching in a twist-boat and chair conformer with either the *re* or *si* face of the alkene coordinated to the yttrium. These starting structures were well minimized using the force field corresponding to **4**, where the equilibrium Y−DA distance is 2.70 Å, with a 700 kcal mol^{-1} Å^{-2} force constant, and the Y−DA−C5 equilibrium angle is 80°, with a 1000 kcal mol^{-1} rad^{-2} force constant. Throughout this work, the force constants for all the force fields are invariant; only the equilibrium geometry changed.

Each independent minimum served as a starting point for searching via a combination of minimization in one of the nine force fields (2.55, 2.70, and 2.85 Å; 70, 80, and 90°) and three cycles of simulated annealing dynamics followed by quenching. Annealed dynamics simulations were run (using the appropriate force field) from 600 to 0.001 K and back in 10 K increments, using isoergic, isochoric summed Verlet dynamics with a time step of 1 fs and 50 steps per temperature increment. The lowest energy step in each of these cycles was saved and quenched with 1500 steps of conjugated gradient minimization. The final quenched conformation of each annealing run was placed in a new force field and the cycle restarted. Each of the four starting points thus contributed 36 members of the initial ensemble, for a total of 144 chelate conformers.

Sixty yttrium pentenyl conformers were generated in which the alkene centroid dummy atom is not bonded to the yttrium. This means that the metal equilibrium geometry is that of a monovacant tetrahedron. Sixteen of the conformers were generated from four starting points by simulated annealing using the approach described above. The remaining 44 conformers were created by torsion randomization of all of the freely rotateable alkyl bonds in the pentenyl chain (Y−C1, C1−C2, C2−C3, C3−C4). These conformers were then minimized by 100 steps of steepest descent, followed by 1500 steps of conjugate gradient.

A superset of the original ensemble was created by searching using the protocol above with eight additional force fields (2.70 and 2.85 Å with 100 and 110°; 3.00 Å with 80, 90, 100, and 110°) for 128 new chelate structures. Sixty additional yttrium pentenyl conformers were also added to this superset, this time with a trigonal planar yttrium equilibrium geometry. The trigonal planar yttrium force field adds two 120.0°, cosine harmonic angle terms to the original, one for the Cp DA−Y-alkyl carbon, with a force constant of 25.4 kcal mol^{-1} rad^{-2}, and the other for the Cp DA−Y−Cp DA, with a force constant of 30.8 kcal mol^{-1} rad^{-2}. The default equilibrium yttrium bond angle was changed to 120.0°, and a 0.0° umbrella term around yttrium was added, with a force constant of 50.0 kcal mol^{-1} rad^{-2}.

Changes in the 2DCPA Program. Several changes have been introduced in the 2DCPA program since the last publication detailing its operation.[20] The most important change to the previously detailed algorithms is in the matrix mathematics used for scaling the observed and calculated apparent (group-by-group) rates. In the fast exchange limit, multiple conformations appear spectroscopically as weighted averages of their NOE rates. 2DCPA is designed to compare the experimental apparent rate to the calculated weighted average apparent rate, where the apparent rates are computed from the eigenvalues and eigenvectors of the apparent intensities. This requires that the experimental apparent rates be transformed to the same scale as the calculated apparent rates. Such scaling may be accomplished by multiplying both experimental and calculated apparent intensity matrices by their respective inverse apparent intensity matrix at time zero. The result is a general asymmetric matrix whose eigenvalues are difficult to compute in a satisfactory way if they must retain their original "identity" with respect to the crosspeaks that gave rise to them. The larger the dynamic range of $\mathbf{I}_0$ (the intensity matrix at time zero), such as when there are 30 equivalent protons, the worse the problem gets. If the eigenvalues and eigenvectors of the asymmetric matrix $\mathbf{I}_t \cdot \mathbf{I}_0^{-1}$ (where $\mathbf{I}_t$ is the intensity matrix at time t) are desired, it can be shown that $(\mathbf{I}_0^{-1})^{1/2}$ can be used as a transformation matrix into the symmetric $(\mathbf{I}_0^{-1})^{1/2} \cdot \mathbf{I}_t \cdot (\mathbf{I}_0^{-1})^{1/2}$ matrix, which can be solved for the same eigenvalues. The original eigenvectors can be recovered using the relations $\mathbf{S} = [(\mathbf{I}_0^{-1})^{1/2}]^{-1} \cdot \mathbf{T}$ and $\mathbf{S}^{-1} = \mathbf{T}^{\mathrm{T}} \cdot (\mathbf{I}_0^{-1})^{1/2}$ where $\mathbf{T}$ is the eigenvector matrix for $(\mathbf{I}_0^{-1})^{1/2} \cdot \mathbf{I}_t \cdot (\mathbf{I}_0^{-1})^{1/2}$ and $\mathbf{S}$ is the eigenvector matrix for $\mathbf{I}_t \cdot \mathbf{I}_0^{-1}$. 2DCPA now avoids diagonalizing asymmetric matrices using these relationships.

We have settled on the use of an error weighting scheme that corresponds to scheme B in ref 20, modified for automatic computation during the 2DCPA run. The weighted error function for observed peaks is shown in eq 1, where $\langle I_i^{\mathrm{obs}} \rangle$ is the mean intensity of the ith peak

$$\sum_i^{\text{all peaks}} \left(\frac{I_i^{\mathrm{obs}} - I_i^{\mathrm{calc}}}{\langle I_i^{\mathrm{obs}} \rangle / \langle I_{\mathrm{min}}{}^{\mathrm{obs}} \rangle} \right)^2 \tag{1}$$

over the time course and $\langle I_{\mathrm{min}}{}^{\mathrm{obs}} \rangle$ is the mean of the smallest peak over the timecourse, giving an inversely proportional weight normalized to 1. Equation 2 is the weighted error function for noisy or absent peaks.

$$\sum_i^{\text{all peaks}} \left(\frac{I_i^{\mathrm{obs}} - I_i^{\mathrm{calc}}}{2} \right)^2 \tag{2}$$

(34) Chevreau, T.; Gault, F. G. *J. Catal.* **1977**, *50*, 124.
(35) Gusel'nikov, L. E.; Polyakov, Yu. P.; Volina, E. A.; Nametkin, N. S. *J. Organomet. Chem.* **1985**, *292*, 189.
(36) States, D. J.; Haberkorn, R. A.; Ruben, D. J. *J. Magn. Reson.* **1982**, *48*, 286.

A routine for solving partially separable minimization problems with upper and lower bounds on the variables replaced the simplex routine previously used for rotational correlation time optimization (Supporting Information Figure 12). It has proved more stable and more efficient, and the termination criteria are more easily controlled. Several functions that had been part of auxiliary programs have been consolidated in the main 2DCPA program, including exhaustive comparison and correlation time optimization. Supporting Information Figure 13 and Supporting Information Table 1 describe the input file contents for the 2DCPA program, including the experimental NOE intensities, the weighting scheme, optimized values for the rotational correlation times (τ), peaks used for τ optimization, and τ optimization averaging. Complete ".csr" format (Quanta) trajectory files of both static ensembles and all 18 ".trj" format (Polygraf) dynamics trajectory files are available on request from Landis.

Dynamic Averaging. The new dynamic averaging facility works by reading in a list of dynamics trajectories, averaging the coordinates in r^{-3} space, and averaging the spherical harmonic contributions of methyl groups in $\cos(\theta)^2$, $\sin(\theta)\cos(\theta)$, and $\sin(\theta)^2$ angular spaces. The resultant averaged structures are stored as either apparent intensities or apparent rates (depending on the exchange limit) for use by 2DCPA. The dynamics simulations for averaging were run (using the appropriate force field) at 220 K to give an average temperature of approximately 170 K (−100 °C). The simulations were isothermal, isochoric summed Verlet dynamics with a time step of 1 fs, recorded every 10 fs for 10 ps. Noncanonical temperature damping with a relaxation time of 0.01 ps and initial temperature assignment *without* doubling the required temperature helped keep the trajectories smooth over the short runs.

Formation of Cp*$_2$Y[η^1,η^2-CH$_2$CH$_2$CH$_2$CH=CH$_2$] (6) from 2 and 1,4-Pentadiene. 2 was prepared in *situ* by hydrogenation of a solution of **3** (11.4 mg, 0.021 mmol) in 0.31 mL of methylcyclohexane-d_{14}. 1,4-Pentadiene (0.019 mmol) was vacuum transferred into the NMR tube, which was sealed and shaken once at −78 °C to produce a bright yellow solution of Cp*$_2$Y[η^1,η^2-CH$_2$CH$_2$CH$_2$CH=CH$_2$] (**6**) (85 ± 5% yield by ^{1}H NMR spectroscopy using CH$_2$(SiMe$_3$)$_2$ as an internal standard vs Cp*). **6** was thermally unstable and was analyzed without isolation by ^{1}H and ^{13}C NMR spectroscopy at −100 °C. ^{1}H NMR (500 MHz, C$_6$D$_{11}$CD$_3$, −100 °C): δ −0.33 (br s, $\omega_{1/2}$ = 22 Hz, YCH$_2$), 1.84 (br s, $\omega_{1/2}$ = 12 Hz, YCH$_2$C*H*$_2$), 1.92 (s, C$_5$Me$_5$), 3.79 (d, J_{cis} = 10.0 Hz, =C*H*H), 5.25 (d, J_{trans} = 17.5 Hz, =CH*H*), 6.58 (br m, CH=), resonance for YCH$_2$CH$_2$C*H*$_2$ obscured by resonance for Cp* ligands. ^{13}C{^{1}H} NMR (126 MHz, C$_6$D$_{11}$CD$_3$, −100 °C): δ 11.6 (s, C$_5$*Me*$_5$), 14.7 (s, YCH$_2$*C*H$_2$), 33.7 (d, J_{YC} = 44.8 Hz, YCH$_2$), 39.4 (s, YCH$_2$-CH$_2$*C*H$_2$), 112.9 (s, =CH$_2$), 116.3 (s, *C*$_5$Me$_5$), 158.1 (s, CH=).

Synthesis of 6 from 2 and Methylenecyclobutane. **2** was prepared *in situ* by hydrogenation of a solution of **3** (18.7 mg, 0.036 mmol) in 0.35 mL of methylcyclohexane-d_{14}. Methylenecyclobutane (0.036 mmol) was vacuum transferred into the NMR tube, which was sealed and shaken once at −78 °C to produce a bright yellow solution of **6** (98 ± 5% yield by ^{1}H NMR spectroscopy using CH$_2$(SiMe$_3$)$_2$ as an internal standard vs. Cp*). ^{1}H NMR (500 MHz, C$_6$D$_{11}$CD$_3$, −100 °C): δ −0.33 (br s, $\omega_{1/2}$ = 22 Hz, YCH$_2$), 1.84 (br s, $\omega_{1/2}$ = 12 Hz, YCH$_2$C*H*$_2$), 1.92 (s, C$_5$Me$_5$), 3.79 (d, J_{cis} = 10.0 Hz, =C*H*H), 5.25 (d, J_{trans} = 17.5 Hz, =CH*H*), 6.58 (br m, CH=), resonance for YCH$_2$-CH$_2$C*H*$_2$ obscured by resonance for Cp* ligands.

^{1}H NMR Analysis of the Hydrogenation of 6. An NMR tube containing a bright yellow solution of **6** (0.036 mmol) in 0.35 mL of methylcyclohexane-d_{14} was sealed under 1 atm of H$_2$ at 77 K and shaken periodically at −78 °C for 15 min. ^{1}H NMR analysis of the resulting solution at −78 °C revealed the formation of **2** (90 ± 5% yield by ^{1}H NMR spectroscopy using SiMe$_3$ resonance of CH$_2$(SiMe$_3$)$_2$ as an internal standard vs Cp*) and pentane (95 ± 5% yield by ^{1}H NMR spectroscopy using SiMe$_3$ resonance of CH$_2$(SiMe$_3$)$_2$ as an internal standard vs Me resonance).

In a similar experiment, low-resolution GC/MS(EI) of the volatile material indicated the presence of pentane (m/z = 72), toluene, and CH$_2$(SiMe$_3$)$_2$. The GC/MS of pentane was identical to that of an authentic sample.

Cp*$_2$Y[η^1,η^2-CH$_2$CHDC(CH$_3$)$_2$CH=CH$_2$] (4-(2-*d*)). Reaction of 3,3-dimethyl-1,4-pentadiene (0.026 mmol) and **2**-*d* (0.027 mmol) using a procedure analogous to that used to form **4** generated Cp*$_2$YCH$_2$-CHDC(CH$_3$)$_2$CH=CH$_2$ (**4**-(2-*d*)) (88 ± 5% yield by ^{1}H NMR spectroscopy using CH$_2$(SiMe$_3$)$_2$ as an internal standard vs Cp*). ^{1}H NMR (500 MHz, C$_6$D$_{11}$CD$_3$, −78 °C): δ −0.44 (br s, YCH$_2$), 1.03 (s, CH$_3$), 1.93 (s, C$_5$Me$_5$), 3.76 (d, J_{cis} = 10.7 Hz, =C*H*H), 5.14 (d, J_{trans} = 17.8 Hz, =CH*H*), 6.78 (dd, J = 17.8, 10.7 Hz, CH=), the broad YCH$_2$-CD*H* resonance was partially obscured by the Cp* resonance.

Cp*$_2$Y[η^1,η^2-CD$_2$CH$_2$CH$_2$CH=CD$_2$] 6-(1,1,5,5-d_4) and Cp*$_2$Y-[η^1,η^2-CH$_2$CH$_2$CD$_2$CH=CD$_2$] 6-(3,3,5,5-d_4). **2** was prepared *in situ* by hydrogenation of a solution of **3** (18.1 mg, 0.035 mmol) in 0.37 mL of methylcyclohexane-d_{14}. 1,4-Pentadiene-1,1,5,5-d_4 (0.037 mmol) was vacuum transferred into the NMR tube, which was sealed and shaken once at −78 °C to produce a bright yellow solution of **6**-1,1,5,5-d_4 and **6**-3,3,5,5-d_4 (93 ± 5% yield by ^{1}H NMR spectroscopy using CH$_2$(SiMe$_3$)$_2$ as an internal standard vs Cp*). The product mixture was thermally unstable and was analyzed without isolation by ^{1}H and ^{13}C NMR spectroscopy at −78 °C. After equilibration, the NMR spectra were consistent with a 1:1 mixture of isomers, and the peaks were assigned as follows. Peaks assigned to **6**-1,1,5,5-d_4. ^{1}H NMR (500 MHz, C$_6$D$_{11}$CD$_3$, −78 °C): δ 1.84 (s, YCD$_2$C*H*$_2$), 1.92 (s, C$_5$Me$_5$), 6.58 (br s, CH=), the resonance YCD$_2$CH$_2$C*H*$_2$ was obscured by the Cp* resonance. ^{13}C{^{1}H} NMR (126 MHz, C$_6$D$_{11}$CD$_3$, −78 °C): δ 11.6 (s, C$_5$*Me*$_5$), 14.7 (s, YCD$_2$*C*H$_2$), 39.1 (s, $\omega_{1/2}$ = 6 Hz, YCD$_2$-CH$_2$*C*H$_2$), 112.3 (p, J_{CD} = 32 Hz, =CD$_2$), 116.2 (s, *C*$_5$Me$_5$), 158.1 (s, CH=), the resonance YCD$_2$ was obscured by the residual solvent peaks. Peaks assigned to **6**-3,3,5,5-d_4. ^{1}H NMR (500 MHz, C$_6$D$_{11}$CD$_3$, −78 °C): δ −0.40 (br s, YCH$_2$) 1.84 (s, YCH$_2$C*H*$_2$), 1.92 (s, C$_5$Me$_5$), 6.58 (br s, CH=). ^{13}C{^{1}H} NMR (126 MHz, C$_6$D$_{11}$CD$_3$, −78 °C): δ 11.6 (s, C$_5$*Me*$_5$), 14.7 (s, YCH$_2$*C*H$_2$), 38.4 (br s, $\omega_{1/2}$ = 32 Hz, YCH$_2$CH$_2$*C*D$_2$, isotope shift = 72 ppb), 112.3 (p, J_{CD} = 32 Hz, =CD$_2$), 116.2 (s, *C*$_5$Me$_5$), 158.1 (s, CH=), the resonance YCH$_2$ was obscured by the residual solvent peaks.

Kinetics of Equilibration of 6-1,1,5,5-d_4 and 6-3,3,5,5-d_4. **2** was prepared *in situ* by hydrogenation of a solution of **3** (15.6 mg, 0.030 mmol) in 0.40 mL of toluene. 1,4-Pentadiene-1,1,5,5-d_4 (0.024 mmol) was vacuum transferred into the NMR tube, which was sealed under 1 atm of H$_2$ at 77 K and shaken occasionally at −78 °C for 24 h. H$_2$ was removed via three freeze−pump−thaw cycles, and the mixtures of **2**, pentane-1,1,5,5-d_4, and pentane-3,3,5,5-d_4 were warmed to room temperature. Assuming an equilibrium ratio of CHD$_2$:CD$_2$ = 3:1, the percentage of **6**-1,1,5,5-d_4 in excess of the equilibrium value was determined from the relative ratio of the CHD$_2$ (δ 0.84) and CD$_2$ (δ 1.13) resonances in the ^{2}H{^{1}H} NMR spectrum. The percent excess **6**-1,1,5,5-d_4 was also determined for reaction mixtures hydrogenated after 15, 30, 60, and 1440 min. The volatile compounds were then analyzed by low-resolution GC/MS. Pentane-d_4: GC/MS(EI) calcd (found) for C$_5$H$_8$D$_4$ (M$^+$) 76 (76). The percentage of **6**-1,1,5,5-d_4 in excess of the equilibrium value was derived from the relative ratio of the propyl fragments at m/e = 45 ((C$_3$H$_5$D$_2$)$^+$) and 47 ((C$_5$H$_3$D$_4$)$^+$) (assuming an equilibrium ratio of (C$_3$H$_5$D$_2$)$^+$:(C$_5$H$_3$D$_4$)$^+$ = 3:1). The first-order rate constant for the approach to equilibrium for the conversion of **6**-1,1,5,5-d_4 to **6**-3,3,5,5-d_4 was determined from plots of ln [% excess **6**-1,1,5,5-d_4] versus time.

Acknowledgment. Financial support from the National Science Foundation is gratefully acknowledged. S.L.H. thanks Procter & Gamble for a fellowship. We thank Dr. Ross A. Widenhoefer and Jennifer J. Fisher for helpful discussions.

Supporting Information Available: ^{1}H NMR spectra of compounds **4**−**6**, NOE spectra of **4** and **5**, drawings of twist-boat and chair conformations of **4** calculated using molecular mechanics, ^{13}C NMR spectra of **6**-1,1,5,5-d_4 and **6**-3,3,5,5-d_4, a kinetic plot for the conversion of **6**-1,1,5,5-d_4 to **6**-3,3,5,5-d_4, further characterization of the molecular mechanics ensemble, operational input data for 2DCPA, and tabular results of exhaustive 2DCPA fitting runs for both static and dynamic ensembles (27 pages). See any current masthead page for ordering and Internet access instructions.

JA9632567